HHS Public Access

Author manuscript

J Am Chem Soc. Author manuscript; available in PMC 2023 November 23.

Published in final edited form as:

J Am Chem Soc. 2022 November 23; 144(46): 21337–21346. doi:10.1021/jacs.2c09580.

Sm(II)-Mediated Proton-Coupled Electron Transfer: Quantifying Very Weak N−H and O−H Homolytic Bond Strengths and Factors Controlling Them

Emily A. Boyd,

Division of Chemistry and Chemical Engineering, California Institute of Technology (Caltech), Pasadena, California 91125, United States

Jonas C. Peters

Division of Chemistry and Chemical Engineering, California Institute of Technology (Caltech), Pasadena, California 91125, United States

Abstract

Coordination of alcohols to the single-electron reductant samarium diiodide (SmI_2) results in substantial O−H bond weakening, affording potent proton-coupled electron transfer (PCET) reagents. However, poorly defined speciation of SmI_2 in tetrahydrofuran (THF)/alcohol mixtures limits reliable thermodynamic analyses of such systems. Rigorous determination of bond dissociation free energy (BDFE) values in such Sm systems, important to evaluating their reactivity profiles, motivates studies of model Sm systems where contributing factors can be teased apart. Here, a bulky and strongly chelating macrocyclic ligand ($(^{t\mathrm{Bu2}}\mathrm{ArOH})_2\mathrm{Me}_2$cyclam) maintains solubility, eliminates dimerization pathways, and facilitates clean electrochemical behavior in a well-defined functional model for the PCET reactivity of Sm^{II} with coordinating proton sources. Direct measurement of thermodynamic parameters enables reliable experimental estimation of the BDFEs in 2-pyrrolidone and MeOH complexes of $((^{t\mathrm{Bu2}}\mathrm{ArO})_2\mathrm{Me}_2\mathrm{cyclam})\mathrm{Sm}^{II}$, thereby revealing exceptionally weak N−H and O−H BDFEs of 27.2 and <24.1 kcal mol^{-1}, respectively. Expanded thermochemical cycles reveal that this bond weakening stems from the very strongly reducing Sm^{II} center and the formation of strong Sm^{III}−alkoxide (and −pyrrolidonate) interactions in the PCET products. We provide a detailed analysis comparing these BDFE values with those that have been put forward for SmI_2 in THF in the presence of related proton donors. We suggest that BDFE values for the latter systems may in fact be

Corresponding Author: Jonas C. Peters − Division of Chemistry and Chemical Engineering, California Institute of Technology (Caltech), Pasadena, California 91125, United States; jpeters@caltech.edu.

Author Contributions

The manuscript was written through contributions of all authors.

Supporting Information

The Supporting Information is available free of charge at https://pubs.acs.org/doi/10.1021/jacs.2c09580.

Experimental procedures; compound characterization data; and additional figures and tables as discussed in the text (PDF)

Accession Codes

CCDC 2195229−2195230 contain the supplementary crystallographic data for this paper. These data can be obtained free of charge via www.ccdc.cam.ac.uk/data_request/cif, or by emailing data_request@ccdc.cam.ac.uk, or by contacting The Cambridge Crystallographic Data Centre, 12 Union Road, Cambridge CB2 1EZ, UK; fax: +44 1223 336033.

Complete contact information is available at: https://pubs.acs.org/10.1021/jacs.2c09580

The authors declare no competing financial interest.

appreciably higher than the system described herein. Finally, protonation and electrochemical reduction steps necessary for the regeneration of the PCET donors from Sm^{III}–alkoxides are demonstrated, pointing to future strategies aimed at achieving (electro)catalytic turnover using Sm^{II}-based PCET reagents.

Graphical Abstract

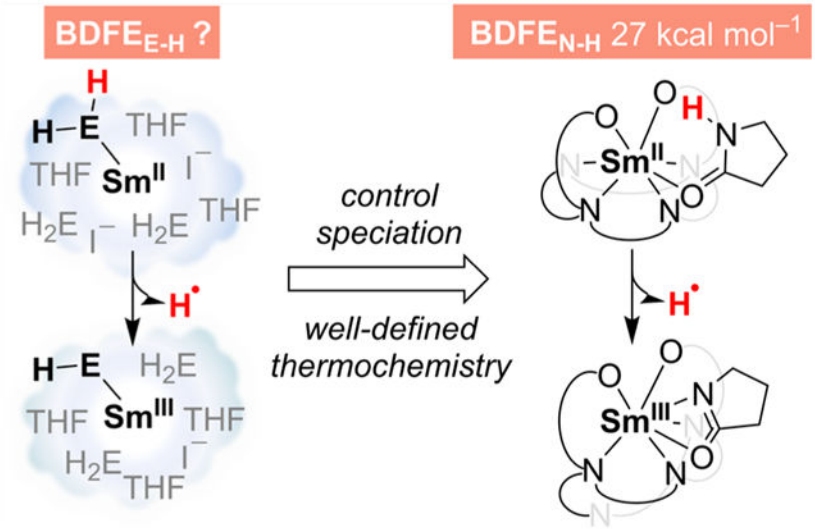

INTRODUCTION

Samarium(II) diiodide (SmI_2) is one of the most versatile and selective single-electron reductants currently available.[1,2] The lability of ligands at the lanthanide center allows for facile variation of the reductant strength and steric profile of Sm(II) by in situ reaction of $SmI_2(THF)_n$ with various additives.[3–5] Additionally, the pronounced oxophilicity of samarium (and the lanthanides in general) affords SmI_2 a strong thermodynamic bias for reactions that form Sm^{III}–O bonds.[6] The combination of these characteristics has resulted in the emergence of SmI_2/alcohol adducts as reductive proton-coupled electron transfer (PCET) reagents.

As illustrated in Figure 1A, the coordination of water (as well as alcohols, secondary amides, or ammonia, generally defined as EH) to SmI_2 yields [Sm^{II}–EH] species capable of PCET (sometimes designated concerted proton-electron transfer (CPET)) to substrates for which initial electron transfer (ET) would be highly endergonic.[7–13] Contrasting other strong reductive PCET reagents, and critical to their efficacy, [Sm^{II}–EH] adducts are curiously stable with respect to the hydrogen evolution reaction (HER).[8]

While the reported PCET reaction profiles of Sm^{II}–EH reagents indicate that coordination to Sm^{II} results in highly significant O− or N−H bond weakening in EH, the ill-defined speciation of [Sm^{II}–EH] has hampered precise quantitation of this effect. For example, the O−H bond dissociation free energy ($BDFE_{O–H}$) of the aqueous Sm^{2+} ion, which can be formulated as $Sm(H_2O)_n^{2+}$, has been most recently estimated as 26 kcal mol^{-1} by Kolmar

and Mayer.[8] However, the degree to which this value can be extended to widely used organic solvents (e.g., in THF, where $[SmI_{2-n}(THF)_m(H_2O)_p]^{n+}$ species will dominate) is unclear; BDFEs typically vary substantially among different complexes of a metal ion.[14] Mayer's 2017 study indeed underscores this dilemma, pointing to the uncertainty in speciation and the insolubility of Sm(III) products as limits on a more precise thermodynamic evaluation of the $BDFE_{O–H}$ for Sm(II) in water/THF mixtures.[8] Knowledge of such values is key to reliable benchmarking of PCET reagent strengths,[14] estimation of chemical overpotentials,[15] and evaluation of available mechanistic pathways.[16]

The $BDFE_{O–H}$ of $SmI_2(H_2O)_n(THF)_m$ has been alternatively constrained as less than or equal to the first $BDFE_{C–H}$ formed in substrates which it can successfully reduce, such as anthracene (~39 kcal mol^{-1}) or an enamine (~31 kcal mol^{-1}, see Figure 1A).[7,8,10,11,17] While a reasonable starting point, the possibility of an uphill initial PCET step cannot be discounted. The driving force for hydrogenation of an alkene substrate is defined by the *average* of the first and second $BDFE_{C–H}$ formed in the reduced substrate, as illustrated in Figure 1A. Therefore, reduction of anthracene to dihydroanthracene, for example, only allows reliable bracketing of the $BDFE_{O–H}$ of $SmI_2(H_2O)_n(THF)_m$ to ≤54.2 kcal mol^{-1} solely based on this thermodynamic argument.[18,19]

An upper bound value can instead be estimated analytically based on a kinetic evaluation of PCET from $SmI_2(H_2O)_n(THF)_m$ to an enamine substrate with $BDFE_{C–H,1}$ = 31 kcal mol^{-1}.[8] A hydrogenation mechanism composed of an initial CPET step (k_1) followed by irreversible consumption of the radical intermediate by a second equivalent of Sm(II) (k_2) is shown in Figure 1A. Based on deuterium labeling studies, which indicate that the initial PCET step is irreversible under the reaction conditions,[8] and by constraining k_2 to values below the diffusion-controlled limit (~10^9 M^{-1} s^{-1}), an upper limit on k_{-1} is estimated to satisfy $k_2[Sm^{II}–OH_2] \gg k_{-1}[Sm^{III}–OH]$ at the lowest $[Sm^{II}–OH_2]$ obtained during the reaction.[20] Combined with an approximate k_1 based on the reported timescale of this conversion,[8,20] we suggest that a reliably deduced conservative *upper bound* for the $BDFE_{O–H}$ of $SmI_2(H_2O)_n(THF)_m$ is 42 ± 1 kcal mol^{-1}. Relatedly, using pyrrolidone (abbreviated herein as PH) instead of H_2O as the Sm^{II}–EH reagent in the reduction of phenanthrene, we estimate a similar *upper bound* for the $BDFE_{N–H}$ in $SmI_2(PH)_n(THF)_m$ as 41 ± 1 kcal mol^{-1}.[10] A detailed discussion of these estimates is provided in the Supporting Information.

While these upper bound estimates are fully consistent with strong EH activation on binding to Sm(II), as yet it is not, from available data at least, possible to discern how close they truly are to the 26 kcal mol^{-1} estimate most recently provided.[8] Given the broad and growing utility of Sm^{II}–EH reagents, and the associated importance of correlating their $BDFE_{E–H}$ values with their reactivity profiles,[21–23] a more quantitative evaluation of Sm^{II}-induced bond weakening is desirable.

To address this challenge, herein, we study a $[Sm^{II}–EH]$ subunit within the bulky, strongly chelating supporting ligand (^{t}Bu2ArOH)$_2$Me$_2$cyclam (1,8-bis(2-hydroxy-3,5-di-*tert*-butylbenzyl)-4,11-dimethyl-1,4,8,11-tetraazacyclotetradecane) reported by Maria et al. (Figure 1B).[24,25] As we show, well-behaved electrochemistry and speciation for this system

enables reliable determination of very low $BDFE_{X–H}$ values (<28 kcal mol^{-1}) for two kinetically stable [Sm^{II}–EH] adducts, and we provide evidence and associated arguments to suggest that these values are likely appreciably lower than those for SmI_2 in THF in the presence of related proton donors. The present model system hence provides a robust benchmark for considering Sm^{II}–EH BDFEs more broadly. Additionally, the chemistry described points to the future possibility of using such systems to drive electrocatalytic reductions via PCET processes.

RESULTS AND DISCUSSION

Redox Chemistry of 1.

Electrochemical reduction of Sm^{III} to Sm^{II} has not been widely explored. For SmI_3 in particular, cases in which it has been demonstrated have required nontraditional electrodes (e.g., Sm metal) and electrolytes (e.g., ionic liquids).[26,27] However, several Sm^{III} complexes supported by bulky multidentate ligands exhibit reversible electrochemical reduction under more typical conditions.[28,29] Cyclic voltammetry (CV) experiments were therefore undertaken to evaluate the facility of $Sm^{III/II}$ redox cycling with the ($^{t\mathrm{Bu2}}$ArO)$_2$Me$_2$cyclam ligand (Figure 2).

Oxidation of the (($^{t\mathrm{Bu2}}$ArO)$_2$Me$_2$cyclam)Sm^{II} complex **1** with one equivalent of thallium hexafluorophosphate yields a pale yellow species with heteronuclear NMR signatures consistent with its assignment as cationic [**2**]PF_6 (Figure 2), a PF_6^- analogue of the known salt [**2**]BPh_4.[25] The CV of [**2**]PF_6 in DME (0.2 M ^{n}Bu$_4$NPF_6) on a glassy carbon electrode reveals a reversible 1e^- reduction at −2.43 V vs $Fc^{+/0}$ (Figure 2, blue) assigned as the $Sm^{III/II}$ couple. **1** exhibits a nearly identical couple at −2.45 V vs $Fc^{+/0}$ (Figure 2, green), supporting assignment of this wave to a $Sm^{III/II}$ redox process.Both **1** and [**2**]PF_6 display peak-to-peak separations smaller than that of the $Fc^{+/0}$ wave under the same conditions, indicative of facile heterogeneous ET kinetics. The reduction potential of cationic [**2**]PF_6 is 170 mV positive of the neutral *tris*-aryloxide Sm^{III} complex reported by Meyer and coworkers.[28]

PCET Reactivity of 1.

To evaluate the ability of **1** to mimic the PCET reactivity observed with SmI_2, we explored its behavior in the presence of protic ligands. The addition of one equivalent of 2-pyrrolidone (PH) to **1** in benzene results in a color change from brown to green, consistent with the coordination of PH to **1** to generate a **1**-PH species.[25] The solution fades to colorless over the course of ca. 3 days, producing H_2 and the oxidized, deprotonated Sm^{III}–pyrrolidonate complex **2**-P in moderate yield (see the SI).

Alternatively, **1**-PH reacts instantaneously with 0.5 equivalents of the styrenyl substrates *trans*-stilbene, 1,1-diphenylethylene (DPE), and tetraphenylethylene to generate hydrogenated products in 83−92% yields (see Scheme 1 and SI). Complex **2**-P, the product of net H release, was isolated as a colorless solid from the reaction of **1**-PH with excess styrene. Its solid-state crystal structure (Figure 3) reveals a sevencoordinate Sm^{III} center in which the pyrrolidonate ligand binds κ^2 and one of the cyclam amine groups is dissociated. Similar flexibility of this ligand has been observed in its complexes of Yb.[24] Diffusion

ordered spectroscopy (DOSY) suggets that **2**-P remains monomeric in the solution phase (Figure S21−S24).

Replacing PH with MeOH results in analogous reactivity. In benzene, the green **1**-MeOH adduct evolves H_2 over the course of ca. 3 days. Alternatively, it can be intercepted by the styrenyl substrates *trans*-stilbene, DPE, and tetraphenylethylene to yield hydrogenated products in high conversion (see the SI). In all cases, the colorless Sm^{III}−OMe complex **2**-OMe is obtained (Figure 3). Single crystals of **2**-OMe were obtained from the reaction of **1**-MeOH with *trans*-stilbene. In the solid state, **2**-OMe is six-coordinate with one of the cyclam amine donors dissociated as in its pyrrolidonate analogue **2**-P.

Electrochemical PCET with [2-PH]$^+$.

The well-behaved electrochemistry of [**2**]PF_6 is conserved upon coordination of PH. Addition of up to 30 equivalents of PH causes the $Sm^{III/II}$ couple of [**2**]PF_6 to shift cathodically, but the wave remains reversible (red trace in Figure 4). This response suggests that PH coordinates to the Sm^{III} center of [**2**]PF_6 to form a more electron-rich [**2**-PH]$^+$ adduct that is reduced to **1**-PH at −2.58 V vs $Fc^{+/0}$. The reversibility of the wave is consistent with the observed kinetic stability of **1**-PH. Similar behavior is observed with the aprotic *N*-methylpyrrolidone (PMe) analogue of PH, and a reversible $Sm^{III/II}$ couple for the [**2**-PMe]$^+$ adduct is assigned at −2.61 V vs $Fc^{+/0}$ (yellow trace).

Addition of DPE to [**2**]PF_6 or to [**2**-PMe]$^+$ does not significantly perturb their respective $Sm^{III/II}$ couples (blue and green traces), indicating that neither **1** nor the more reducing **1**-PMe reacts with DPE on the CV timescale. However, addition of 20 equivalents of DPE to [**2**-PH]$^+$ (purple trace) results in loss of reversibility in the $Sm^{III/II}$ couple. These data show that the presence of an N−H (instead of N−Me) bond in the electrochemically generated **1**-PH adduct facilitates its reaction with DPE.

Analysis of the evolution of the cathodic peak potential $E_{p,c}$ with the scan rate enables extraction of the observed rate constant k_+ for the reaction of **1**-PH with DPE under pseudo first-order conditions (see the SI).[30] The observed rate constant k_+ increases linearly with increasing concentration of DPE (Figure 4 inset). The proton-coupled reduction of DPE by **1**-PH is therefore first order in the substrate with a rate constant of 44 M^{-1} s^{-1}. Repeating this measurement with 2-pyrrolidone-d_1 gives a k_H/k_D ratio of 2.3. This kinetic isotope effect is similar to the value of 2.1 reported for PCET from SmI_2/H_2O to anthracene that has been assigned as concerted.[7] We note that a stepwise PCET mechanism in the present case, comprising an uphill initial ET step followed by fast PT, cannot be discounted because of the very negative reduction potential of **1**-PH.

Thermochemical Measurements.

The reactivities of **1**-PH and **1**-MeOH are suggestive of coordination-induced bond weakening akin to that observed with SmI_2 and alcohol or amide ligands.[7–10] As discussed above, ill-defined SmI_2/alcohol mixtures are not conducive to quantitative measurements of coordination-induced bond weakening at Sm^{II} owing, for example, to ill-defined speciation and solubility issues. The comparatively tractable system **1**-PH provides a

platform to directly interrogate this issue. The $BDFE_{N-H}$ of **1**-PH was determined using the thermodynamic cycle highlighted in purple in Scheme 2, which requires determination of the $Sm^{III/II}$ reduction potential and the pK_a of [**2**-PH]$^+$.

We have collected all thermochemical data in acetonitrile because of the availability of reliable thermodynamic parameters and pK_a scales in this solvent.[14,31] The crystal structure of [**2**]BPh_4 obtained from an MeCN solution contains bound MeCN, and NMR data are consistent with MeCN coordination in the solution phase to form a [**2**-NCMe]$^+$ adduct.[25] The CV of [**2**-NCMe]PF_6 in MeCN (0.1 M ^{n}Bu$_4$NPF_6) is reversible with $E_{1/2}(Sm^{III/II})$ = −2.51 V vs $Fc^{+/0}$ (Figure 5, blue trace). Titration of [**2**-NCMe]PF_6 with PH results in a negative shift in the cathodic wave, consistent with the displacement of MeCN by the more strongly donating amide. The CV profile remains unchanged past 15 equiv PH, suggesting that all of [**2**]PF_6 is ligated by PH at this concentration. Increasing the concentration of PH also results in some loss of reversibility which we attribute to the reduction of acetonitrile solvent by **1**-PH.[32] However, there is a slight anodic return wave which becomes more pronounced at faster scan rates. This feature was used to estimate the $E_{1/2}(Sm^{III/II})$ of [**2**-PH]$^+$ as −2.61 V vs $Fc^{+/0}$.

The pK_a of [**2**-PH]$^+$ was measured using 1H NMR spectroscopic titration measurements. Addition of three equivalents PH to [**2**-NCMe]PF_6 in CD_3CN generates [**2**-PH]$^+$ in situ (see the SI). The equilibrium binding constant for the formation of [**2**-PH]$^+$ was determined to be (1.7 ± 0.7) × 10^3 (reaction (i) in Scheme 3). [**2**-PH]$^+$ establishes a rapid proton-transfer equilibrium with the base 1,8-diazabicyclo[5.4.0]undec-7-ene (DBU, pK_a = 24.3 in CH_3CN)[31] to form **2**-P and [DBUH]$^+$ (Scheme 3, reaction (ii)). Analysis of the chemical shifts of the equilibrium mixture (see the SI) yields the desired pK_a of [**2**-PH]$^+$ as 25.4 ± 0.2. Control reactions between DBU and [**2**-NCMe]PF_6 or a mixture of [**2**-NCMe]PF_6 and PMe revealed no interaction between these reagents in the absence of an acidic proton, ruling out DBU coordination as a competitive pathway. With these data, along with the value of C_G in CH_3CN (52.6 kcal mol^{-1}),[14] the experimental $BDFE_{N-H}$ of **1**-PH is determined from eq 1 in Scheme 2 to be 27.2 ± 0.3 kcal mol^{-1}.

The $BDFE_{O-H}$ of **1**-MeOH could not be determined with eq 1 because a $Sm^{III/II}$ couple could not be definitively assigned for [**1**-MeOH]$^+$. To reliably estimate $BDFE_{O-H}$ for the MeOH adduct of Sm^{II}, we employed the alternative thermodynamic cycle highlighted in purple in the right side of Scheme 2 and represented by eq 5. In CD_3CN, binding of MeOH to [**2**-NCMe]PF_6 is negligible. The effective pK_a of [**2**-NCMe]PF_6 in the presence of MeOH (p*K*a,eff) was therefore determined by titration measurements. Addition of diisopropylamine (pK_a =18.8 in CH_3CN)[31] or quinuclidine (pK_a = 19.7 in CH_3CN) to a mixture of [**2**]PF_6 and MeOH results in ^{1}H NMR shifts attributed to the proton-transfer equilibria in reactions (iii) and (iv) shown in Scheme 3. The desired p*K*a,eff value for the combination of [**2**-NCMe]PF_6 and MeOH can be extracted from either reaction as 19.9 ± 0.2 (see the SI). As with DBU, neither amine interacts with [**2**-NCMe]PF_6 in the absence of MeOH.

The binding affinity of MeOH to **1** ($\Delta G°$Sm(II)-MeOH) is bracketed by cross-reference to the cycle highlighted in green in Scheme 2 for the affinity of PH to **1** ($\Delta G°$Sm(II)-PH; eq 2). Because MeOH has a lower affinity for Sm(II) compared to PH, $\Delta G°$Sm(II)-MeOH must be

more positive (i.e., $\Delta G°$Sm(II)-MeOH> −2.1 kcal mol^{-1}; eq 4). A reliable upper limit of ≤ 24.1 kcal mol^{-1} is therefore determined for the $BDFE_{O-H}$ of **1**-MeOH.

Origins of Bond Weakening.

Coordination of PH or MeOH to **1** yields two of the strongest reductive PCET reagents whose BDFE values have been systematically characterized.[14,33,34] The N−H bond in **1**-PH is weakened by ca. 69 kcal mol^{-1} from that of free PH,[10] which for comparison is 13 kcal mol^{-1} more weakened than the N−H bonds in a Mo^{I}–NH_3 complex previously described by Chirik and co-workers as a fascinating example of dramatic coordination-induced bond weakening.[35,36] Similarly, O−H bond weakening in **1**-MeOH is more pronounced than that in $Cp_2Ti(OH_2)$ complexes by at least ~10 kcal mol^{-1}.[14,37,38] The magnitude of the $BDFE_{N-H}$ of **1**-PH is also 10 kcal mol^{-1} weaker than the N−H bond we have measured for *N,N*-dimethylanilinium-appended cobaltocene, which contained the weakest experimentally determined $BDFE_{N-H}$ that had been reported to date.[39]

It is instructive to next consider the origins of the dramatic bond weakening determined herein. First, we note that the bulk of the difference in $BDFE_{N-H}$ between free pyrrolidone and **1**-PH is *independent of coordination*. Bond weakening can be regarded as an increased capacity to give up H$^{\cdot}$, or equivalently, a proton and an electron. For example, homolytic cleavage of the N−H bond in PH is thermodynamically equivalent to deprotonation to form pyrrolidonate, followed by oxidation. Coupling deprotonation of PH to facile oxidation of any strong reductant such as **1** is thermodynamically much more favorable. This is formalized by defining the "effective" BDFE, $BDFE_{eff}$, which describes the net removal of H from a noninteracting combination of reductant and acid (eq 7). The $BDFE_{eff}$ of the Sm^{II}/EH combinations explored here can be determined by the insertion of the reduction potential of [**2**-NCMe]PF_6 (–2.51 V) and the pK_a of PH (estimated as 37 in CH_3CN)[40,41] or MeOH (~39)[42] into eq 7 to yield values of 45 and 48 kcal mol^{-1} for **1**/PH and **1**/MeOH, respectively. These values represent bond weakening of ~50 kcal mol^{-1} compared to free PH and MeOH. The same values could be obtained with PH or MeOH and any reductant with $E° \approx -2.5$ V.

However, unlike some PCET reagents composed of synthetically linked but electronically decoupled ET and PT mediators,[39,43] there is a significant difference between the $BDFE_{eff}$ and $BDFE_{X-H}$ values for **1**/PH and **1**/MeOH. As laid out in Scheme 4, the difference, ΔBDFE, can be decomposed into the binding energy of EH to Sm(II) ($\Delta G°$Sm(II)−EH) and the affinity of E$^-$ for Sm(III)$^+$ ($\Delta G°_{Sm(III)-E}$). A larger ΔBDFE is obtained with a *weaker* Sm^{II}–EH association (more positive $\Delta G°_{Sm(II)-EH}$) and a *stronger* Sm^{III}–E interaction (more negative $\Delta G°_{Sm(III)-E}$).

Because $\Delta G°_{Sm(II)-EH}$ is estimated to be close to thermoneutral for the systems described here (−2.1 kcal mol^{-1} and > −2.1 kcal mol^{-1} for PH and MeOH binding to **1**, respectively), the Sm^{III}–E interactions dominate the ΔBDFE. $\Delta G°$Sm(III)−E values were determined using the orange-highlighted thermodynamic cycles and eqs 3 and 6 in Scheme 2 as −20 kcal mol^{-1} for **2**-P and −26 kcal mol^{-1} for **2**-OMe. The stronger affinity of OMe^- for Sm^{III} results in the slightly lower $BDFE_{O-H}$ of **1**-MeOH, despite the **1**/MeOH pair having

the higher $BDFE_{eff}$ because of the somewhat weaker acidity of MeOH compared to PH. Rational modulation of the BDFE of [Sm^{II}−EH] species based on the pK_a of free EH is therefore not straightforward, as the Sm^{III} binding affinities of different E^- anions are not readily predictable.

An alternative strategy for BDFE weakening that emerges from Scheme 4 is to *decrease* the affinity of EH for Sm^{II}. This conclusion is somewhat counterintuitive; indeed, while MeOH has a lower affinity for SmI_2 in THF than H_2O, SmI_2 is more prone to PCET reactivity in the presence of H_2O than MeOH despite the likely similarity in $\Delta G°_{Sm(III)-E}$ for methoxide and hydroxide. We attribute this discrepancy to two possible origins: first, if EH is such a poor donor ligand that a [Sm^{II}−EH] complex forms only in a very low equilibrium concentration, PCET (which typically requires pre-association of at least two components of the reaction)[14] cannot occur at appreciable rates. Second, EH with lower affinity for Sm^{II} typically produces a less pronounced cathodic shift in $Sm^{III/II}$ reduction potential.[4] This effect is likely to counteract a more positive $\Delta G°$Sm(II)−EH in eqs 7 and 8 (vide infra), resulting in a smaller degree of net bond weakening, further illustrating the complex interdependence of parameters that determine the $BDFE_{X-H}$ of [Sm^{II}−EH] reagents.

Implications for SmI_2-Based PCET Reagents.

Because the saturated coordination sphere of [**1**-PH] is unlikely to vary between THF and MeCN solvents, the $BDFE_{N-H}$ of **1**-PH is expected to be very similar in these two solvents.[14] This assumption enables comparison of the $BDFE_{N-H}$ of **1**-PH determined here as 27.2 kcal mol^{-1} to the reported $BDFE_{N-H}$ of the PH adduct of SmI_2 in THF (SmI_2 (THF) n(*PH*)$_m$, 25.3 kcal mol^{-1}), suggesting that the $BDFE_{X-H}$ of [Sm^{II}−EH] species is nearly invariable with the coordination sphere of Sm^{II}. However, as laid out in the Introduction, the known PCET reactivity of $SmI_2(THF)_n$(*PH*)$_m$ could still be accessed with a $BDFE_{N-H}$ as high as 41 kcal mol^{-1}, leading to the inverse conclusion that [Sm^{II}−EH] BDFE's are highly sensitive to supporting ligands. In this section, we reason that the latter conclusion is more likely.

The oxidation of SmI_2 shifts negative by up to 0.77 V in THF with the addition of excess PMe.[4] As shown in Figure 4, PMe and PH coordination have similar effects on the SmIII/II reduction potential of [**2**]PF_6. The $Sm^{III/II}$ reduction potential of $SmI_2(THF)_n$(*PH*)$_m$ can therefore be approximated as ~ −2.2 V vs $Fc^{+/0}$,[44] 0.4 V positive of that of **1**-PH (−2.58 V vs $Fc^{+/0}$ in DME). The relationship between $BDFE_{X-H}$ and $E°$ varies dramatically across different classes of metal-bound ligands.[14] For example, for a series of [Cu^{II}−OH_2] complexes with varied electron donating/withdrawing properties in the supporting ligand backbone, a 0.38 V increase in $E°$ is offset by a decrease in pK_a such that the $BDFE_{O-H}$ of the aquo ligand increases by only 3 kcal mol^{-1}.[45] By contrast, the $BDFE_{N-H}$ of a Ru^{II}-bound imidazole fragment increases by almost 18 kcal mol^{-1} with the incorporation of electron-withdrawing groups in the ancillary ligands that shift $E°$ positive by 0.93 V but have virtually no effect on the pK_a.[46]

We posit that the pK_a of a [Sm^{III}−EH]$^+$ complex is unlikely to depend strongly on the supporting ligands (consequently, $BDFE_{X-H}$ should most strongly correlate with $E°$ ($Sm^{III/II}$)).For a given EH, the pK_a of [Sm^{III}−EH]$^+$ is dictated by the binding energy of

EH to $Sm(III)^+$ ($\Delta G°Sm(III)-EH$) and the affinity of E^- for $Sm(III)^+$ ($\Delta G°Sm(III)-E$) (eq 3). When the former becomes more favorable, the pK_a increases. It seems unlikely that a $Sm(III)^+$ complex with a bulky, strongly chelating ligand (e.g., [**2**]PF_6) would have a higher affinity for EH than a complex with more labile monodentate ligands (e.g., $SmI_2(THF)_n(PH)_m$), so the predominant mechanism by which increasing $E°$ could be counterbalanced by decreasing pK_a correlates with the variation of $\Delta G°_{Sm(III)-E}$.

Farran and Hoz measured the strength of $\Delta G°_{Sm(III)-E}$ between $[SmI_2(THF)_n]^+$ and the benzophenone ketyl radical anion (Ph_2CO^-) as −19 kcal mol^{-1} based on inner-sphere ET equilibria.[6] We therefore sought to access this value with $[\mathbf{2}]^+$ in order to make a direct comparison of $\Delta G°Sm(III)-E$ values for the same Sm^{III}–alkoxide fragment in these drastically different coordination spheres.

Reduction of benzophenone by **1** is downhill even in the absence of additional driving force from alkoxide binding ($\Delta E°$ = 150 mV in DME). Accordingly, the addition of 1 equiv of benzophenone to 1 mM **1** in DME containing 0.2 M $^n Bu_4NPF_6$ results in an immediate color change from dark green to dark purple. The open circuit potential of the solution shifts from −2.5 to −1.7 V vs $Fc^{+/0}$. Sweeping positive from open circuit reveals an irreversible anodic wave with $E_{p,a}$ = −1.62 V vs $Fc^{+/0}$ (Figure 6A, red trace). The same wave is present in the CV of 1 mM [**2**]PF_6 with 1 equiv of benzophenone (Figure S31). In both systems, the anodic wave shifts positive and gains reversibility with increasing benzophenone concentration. Beyond 10 mM benzophenone, the shift in $E_{1/2}$ is linear with log([benzophenone]) with a slope of 60.8 mV/dec (Figure 6A).

These data are consistent with the assignment of the new anodic feature to the oxidation of a Sm^{III}–$OCPh_2$ species (**2**-$OCPh_2$) generated in situ from the reaction of **1** and benzophenone (Figure 6B, equilibrium (v)). The oxidation is coupled to benzophenone dissociation. At high [benzophenone], the reverse process becomes fast, giving rise to the return cathodic wave corresponding to benzophenone coordination and reduction. In this concentration regime, the system can be approximated as Nernstian and is described by eq 10.

The intercept of the plot of log([benzophenone)] vs $E_{1/2}$ provides $E°$ for the net equilibrium process as −1.52 V vs $Fc^{+/0}$. Using the Hess cycle in Figure 6B and eq 11, the summation of this reaction with the reduction of benzophenone (−2.28 V vs $Fc^{+/0}$ in DME with 0.2 M $^n Bu_4NPF_6$ on glassy carbon, Figure S30) predicts $\Delta G°_{Sm(III)-E}$ for **2**-$OCPh_2$ as −17.5 kcal mol^{-1}. The Sm^{III}– alkoxide interaction strengths in **2**-$OCPh_2$ and the analogous SmI_2-based species, formulated for simplicity as $I_2(THF)_nSm-OCPh_2$, are therefore of very similar magnitude, despite the 1 V difference in the reduction potential of the Sm^{II} reagents. Furthermore, while the simplified representation of $I_2(THF)_nSm-OCPh_2$ does not account for any rapid dimerization or ligand scrambling equilibria that might occur at this state, these processes (if they exist) are contained in the reported $\Delta G°Sm(III)-E$ value, leading to a possible *overestimation* of the interaction strength (more negative $\Delta G°Sm(III)-E$). Because the much less labile coordination sphere of **1** makes it less prone to such equilibria, the $\Delta G°Sm(III)-E$ for the two [Sm^{III}–$OCPh_2$] species may be even more comparable.

Based on this comparison, we can deduce that P^- should have a similar affinity for $[\mathbf{2}]^+$ and $[SmI_2(THF)_n(PH)_{m-1}]^+$, implying that the difference in reduction potentials between **1**-PH and $SmI_2(THF)_n(PH)_m$ is unlikely to be canceled out by an opposite difference in pK_a. This conclusion is consistent with evidence suggesting that $SmBr_2$, a substantially stronger reductant than SmI_2, induces greater O−H bond weakening in THF/H_2O mixtures.[47] As a result, we suspect that the $BDFE_{N-H}$ of $SmI_2(THF)_n(PH)_m$ is closer to 35 than 25 kcal mol^{-1}. Importantly, this analysis does not account for additional driving force for the loss of $H^{\cdot}$ from $SmI_2(THF)_n(PH)_m$ gained from oligomerization or precipitation. However, it does motivate further development of [Sm^{II}−EH]-based PCET reagents whose $BDFE_{X-H}$ values can be tuned by $E°$.

Considerations for Sm-Mediated Electrocatalysis.

Despite the versatile role Sm-mediated reductions serve in synthesis, such systems to date have overwhelmingly required the use of stoichiometric equivalents of Sm. It would be attractive to develop (electro)catalytic reductions mediated via $Sm^{III/II}$ redox chemistry.

In the course of the thermochemical studies presented above we have demonstrated the hypothetical steps needed to regenerate [Sm^{II}−EH] from [Sm^{III}−E] (Scheme 5). PCET from **1**-PH (step 1) generates **2**-P, which is monomeric and soluble in organic solvents, unlike the multimeric [Sm^{III}−E] products obtained from SmI_2/EH in the absence of a bulky supporting ligand.[15] **2**-P can be reversibly protonated by $[DBUH]^+$ in MeCN to generate $[\mathbf{2}\text{-PH}]^+$ (step 2). This demonstration of selective proton transfer to Sm^{III}−alkoxides is of particular note, as the cleavage of strong f-element-oxygen bonds has been cited as the primary barrier to many possible catalytic transformations.[48] Finally, the chelating ligand supports reversible electrochemical reduction back to the Sm^{II} state **1**-PH (step 3).

Attempts to integrate the individual steps in Scheme 5 into a one-pot electrocatalytic reaction have thus far been unsuccessful because of rapid electrode-mediated HER with the acids used in the protonation step ($[DBUH]^+$, alkylammoniums) at the negative potentials required to access the relevant $Sm^{III/II}$ couples. Identification of an electrode/acid combination with slow electrode-mediated HER kinetics is hence desirable toward realizing Scheme 5. However, we note that the generation of species with $BDFE_{X-H}$ < 28 kcal mol^{-1} by successive protonation and electrochemical reduction steps necessitates holding the electrode at a > 1 V overpotential relative to the thermodynamic HER potential of the required acid. Few acids circumvent electrode-mediated HER at such high overpotentials.[49] Therefore, tuning the $BDFE_{X-H}$ of the [Sm^{II}−EH] species to somewhat *higher* values (> 30 kcal mol^{-1}) may be prudent to expand the acid and electrode combinations that could serve to regenerate the PCET donor without substantial background HER.[39]

CONCLUSIONS

To close, the ((^{t}Bu2ArO)$_2$Me$_2$cyclam)Sm^{II} complex **1** binds 2-pyrrolidone or MeOH to generate remarkably strong reductive PCET reagents. The well-defined nature of these complexes, as well as their oxidized and deprotonated congeners, enables direct measurement of thermodynamic parameters necessary to reliably estimate their $BDFE_{X-H}$ values as 27.2 kcal mol^{-1}, and <24.1 kcal mol^{-1},and we provide evidence and arguments

to suggest that these values are likely appreciably weaker than those derived from SmI_2 in THF in the presence of related proton donors. Nevertheless, these complexes cement the view that Sm^{II} coordination induces the most significant bond weakening reported to date. The origins of this effect lie in the reductant strength of Sm^{II} and in the very strong Sm^{III}– alkoxide (or −pyrrolidonate) interactions in the PCET products. While $Sm^{III/II}$ redox potentials vary dramatically with the donor strength of ancillary ligands, we demonstrate that ionic Sm^{III}–alkoxide bond strengths are relatively insensitive to the makeup of the inner coordination sphere, pointing to strategies for rationally tuning [Sm^{II}–EH] BDFE values via $E°$. The detailed thermochemical description of electron, proton, and hydrogen atom transfer at samarium presented here serves as a foundation for developing samarium-mediated (electro)catalytic PCET, a reaction with broad potential utility both in organic synthesis and smallmolecule reduction.

Supplementary Material

Refer to Web version on PubMed Central for supplementary material.

ACKNOWLEDGMENTS

E.A.B. acknowledges the NSF for support via a Graduate Research Fellowship (Grant No. DGE-1745301). The Beckman Institute at Caltech supports the X-ray crystallography facility. This study was supported by funding through the NIH (GM070757).

REFERENCES

(1). Girard P; Namy JL; Kagan HB Divalent lanthanide derivatives in organic synthesis. 1. Mild preparation of samarium iodide and ytterbium iodide and their use as reducing or coupling agents. J. Am. Chem. Soc 1980, 102, 2693–2698.

(2). Szostak M; Fazakerley NJ; Parmar D; Procter DJ Cross-coupling reactions using samarium(II) iodide. Chem. Rev 2014, 114, 5959–6039. [PubMed: 24758360]

(3). Szostak M; Procter DJ Beyond samarium diiodide: vistas in reductive chemistry mediated by lanthanides(II). Angew. Chem., Int. Ed 2012, 51, 9238–9256.

(4). Shabangi M; Sealy JM; Fuchs JR; Flowers RA The effect of cosolvent on the reducing power of SmI_2 in tetrahydrofuran. Tetrahedron Lett. 1998, 39, 4429–4432.

(5). Shabangi M; Flowers RA Electrochemical investigation of the reducing power of SmI_2 in THF and the effect of HMPA cosolvent. Tetrahedron Lett. 1997, 38, 1137–1140.

(6). Farran H; Hoz S Quantifying the electrostatic driving force behind SmI_2 reductions. Org. Lett 2008, 10, 4875–4877. [PubMed: 18855400]

(7). Chciuk TV; Flowers RA Proton-coupled electron transfer in the reduction of arenes by SmI_2−water complexes. J. Am. Chem. Soc2015, 137, 11526–11531. [PubMed: 26273964]

(8). Kolmar SS; Mayer JM SmI2(H2O)n reduction of electron rich enamines by proton-coupled electron transfer. J. Am. Chem. Soc 2017, 139, 10687–10692. [PubMed: 28718640]

(9). Chciuk TV; Anderson WR; Flowers RA Proton-coupled electron transfer in the reduction of carbonyls by samarium diiodide−water complexes. J. Am. Chem. Soc 2016, 138, 8738–8741. [PubMed: 27367158]

(10). Chciuk TV; Li AM; Vazquez-Lopez A; Anderson WR; Flowers RA Secondary amides as hydrogen atom transfer promoters for reactions of samarium diiodide. Org. Lett 2017, 19, 290–293. [PubMed: 28001419]

(11). Ramírez-Solís A; Boekell NG; León-Pimentel CI; Saint-Martin H; Bartulovich CO; Flowers RA Ammonia solvation vs aqueous solvation of samarium diiodide. A theoretical and experimental

approach to understanding bond activation upon coordination to Sm(II). J. Org. Chem 2022, 87, 1689–1697. [PubMed: 34775764]

(12). Bartulovich CO; Flowers RA Coordination-induced O−H bond weakening in Sm(II)-water complexes. Dalton Trans. 2019, 48, 16142–16147. [PubMed: 31549703]

(13). Boekell NG; Flowers RA Coordination-induced bond weakening. Chem. Rev 2022, 122, 13447–13477. [PubMed: 35900048]

(14). Agarwal RG; Coste SC; Groff BD; Heuer AM; Noh H; Parada GA; Wise CF; Nichols EM; Warren JJ; Mayer JM Free energies of proton-coupled electron transfer reagents and their applications. Chem. Rev 2022, 122, 1–49. [PubMed: 34928136]

(15). Ashida Y; Arashiba K; Nakajima K; Nishibayashi Y Molybdenum-catalysed ammonia production with samarium diiodide and alcohols or water. Nature 2019, 568, 536–540. [PubMed: 31019315]

(16). Ashida Y; Arashiba K; Tanaka H; Egi A; Nakajima K; Yoshizawa K; Nishibayashi Y Molybdenum-catalyzed ammonia formation using simple monodentate and bidentate phosphines as auxiliary ligands. Inorg. Chem 2019, 58, 8927–8932. [PubMed: 31247822]

(17). BDFEC-H values for anthracene and the enamine determined by subtracting the entropy of H·solvation (TS°(H·)solv = 6.4 kcal mol−1) from reported BDE values according to ref 14.

(18). Stein SE; Brown RL Prediction of carbon-hydrogen bond dissociation energies for polycyclic aromatic hydrocarbons of arbitrary size. J. Am. Chem. Soc 1991, 113, 787–793.

(19). Luo Y-R Comprehensive Handbook of Chemical Bond Energies; Taylor and Francis Group, LLC: Boca Raton, FL, 2007; p 51.

(20). Mayer and coworkers report that the reaction of a 0.024 M solution of the enamine substrate with 0.072 M SmI2 and 3.6 M H2O is complete in 600 s. Because SmI2 is used in excess, the minimum concentration of [SmII-OH2] is estimated as 0.024 M (after all substrate has been consumed). The average reaction velocity is 4 × 10−5 M s−1. Assuming a first order dependence on Sm(II) and substrate, the rate constant k is estimated as 2 × 10−2 M−1 s−11. The Supporting Information contains an estimate of k1 for this reaction from a more rigorous integrated rate law expression, but the ultimate bracketed BDFE is relatively insensitive to this estimate.

(21). Chalkley MJ; Peters JC Relating N−H bond strengths to the overpotential for catalytic nitrogen fixation. Eur. J. Inorg. Chem 2020, 2020, 1353–1357. [PubMed: 33071628]

(22). Tarantino KT; Liu P; Knowles RR Catalytic ketyl-olefin cyclizations enabled by proton-coupled electron transfer. J. Am. Chem. Soc 2013, 135, 10022–10025. [PubMed: 23796403]

(23). Park Y; Kim S; Tian L; Zhong H; Scholes GD; Chirik PJ Visible light enables catalytic formation of weak chemical bonds with molecular hydrogen. Nat. Chem 2021, 13, 969–976. [PubMed: 34253889]

(24). Maria L; Santos IC; Alves LG; Marçalo J; Martins AM Rare earth metal complexes anchored on a new dianionic bis(phenolate)dimethylaminecyclam ligand. J. Organomet. Chem 2013, 728, 57–67.

(25). Maria L; Soares M; Santos IC; Sousa VR; Mora E; Maralo J; Luzyanin KV A novel samarium(II) complex bearing a dianionic bis(phenolate)cyclam ligand: synthesis, structure and electron-transfer reactions. Dalton Trans. 2016, 45, 3778–3790. [PubMed: 26818107]

(26). Sun L; Sahloul K; Mellah M Use of electrochemistry to provide efficient SmI2 catalytic system for coupling reactions. ACS Catal. 2013, 3, 2568–2573.

(27). Arashiba K; Kanega R; Himeda Y; Nishibayashi Y Electrochemical reduction of samarium triiodide into samarium diiodide. Chem. Lett 2020, 49, 1171–1173.

(28). Halter DP; Palumbo CT; Ziller JW; Gembicky M; Rheingold AL; Evans WJ; Meyer K Electrocatalytic H_2O reduction with f-elements: mechanistic insight and overpotential tuning in a series of lanthanide complexes. J. Am. Chem. Soc 2018, 140, 2587–2594. [PubMed: 29378127]

(29). Veauthier JM; Schelter EJ; Carlson CN; Scott BL; Re RED; Thompson JD; Kiplinger JL; Morris DE; John KD Direct comparison of the magnetic and electronic properties of samarocene and ytterbocene terpyridine complexes. Inorg. Chem 2008, 47, 5841–5849. [PubMed: 18540594]

(30). Savéant J-M Elements of Molecular and Biomolecular Electrochemistry; John Wiley & Sons, Inc: Hoboken, New Jersey, 2006; pp 81–83.

(31). Tshepelevitsh S; Kütt A; Lõkov M; Kaljurand I; Saame J; Heering A; Plieger PG; Vianello R; Leito I On the basicity of organic bases in different media. Eur. J. Org. Chem 2019, 2019, 6735–6748.

(32). Prasad E; Flowers RA Mechanistic impact of water addition to SmI_2: consequences in the ground and transition state. J. Am. Chem. Soc 2005, 127, 18093–18099. [PubMed: 16366561]

(33). Chalkley MJ; Oyala PH; Peters JC Cp* noninnocence leads to a remarkably weak C−H bond via metallocene protonation. J. Am. Chem. Soc 2019, 141, 4721–4729. [PubMed: 30789720]

(34). Schild DJ; Drover MW; Oyala PH; Peters JC Generating potent C−H PCET donors: ligand-induced Fe-to-ring proton migration from a Cp^*Fe^{III}−H complex demonstrates a promising strategy. J. Am. Chem. Soc 2020, 142, 18963–18970. [PubMed: 33103877]

(35). Bezdek MJ; Guo S; Chirik PJ Coordination-induced weakening of ammonia, water, and hydrazine X−H bonds in a molybdenum complex. Science 2016, 354, 730–733. [PubMed: 27846601]

(36). The literature BDFEX-H values originally determined using the Bordwell equation have been adjusted here by the recently reported correction to the CG value in acetonitrile (ref 14.).

(37). Cuerva JM; Campaña AG; Justicia J; Rosales A; Oller-López JL; Robles R; Cárdenas DJ; Buñuel E; Oltra JE Water: the ideal hydrogen-atom source in free-radical chemistry mediated by Ti^{III} and other single-electron-transfer metals. Angew. Chem., Int. Ed 2006, 45, 5522–5526.

(38). This value is based on the gas-phase BDFEO-H of MeOH reported as 96.4 kcal mol−1 (ref 14).

(39). Chalkley MJ; Garrido-Barros P; Peters JC A molecular mediator for reductive concerted proton-electron transfers via electrocatalysis. Science 2020, 369, 850–854. [PubMed: 32792399]

(40). The pKa of PH was estimated in MeCN using the solvent conversion equations developed by Leito et al (ref 41) and the pKa of PH in DMSO: Bordwell, F. G. Equilibrium acidities in dimethyl sulfoxide solution. Acc. Chem. Res 1988, 21, 456–463.

(41). Kütt A; Tshepelevitsh S; Saame J; Lõkov M; Kaljurand I; Selberg S; Leito I Strengths of acids in acetonitrile. Eur. J. Org. Chem 2021, 2021, 1407–1419.

(42). Felton GAN; Vannucci AK; Okumura N; Lockett LT; Evans DH; Glass RS; Lichtenberger DL Hydrogen generation from weak acids: electrochemical and computational studies in the [(η5-C5H5)Fe(CO)2]2 system. Organometallics 2008, 27, 4671–4679.

(43). Manner VW; Mayer JM Concerted proton−electron transfer in a ruthenium terpyridyl-benzoate system with a large separation between the redox and basic sites. J. Am. Chem. Soc 2009, 131, 9874–9875. [PubMed: 19569636]

(44). Enemærke RJ; Hertz T; Skrydstrup T; Daasbjerg K Evidence for ionic samarium(II) species in THF/HMPA solution and investigation of their electron-donating properties. Chem. -Eur. J 2000, 6, 3747–3754. [PubMed: 11073245]

(45). Dhar D; Yee GM; Spaeth AD; Boyce DW; Zhang H; Dereli B; Cramer CJ; Tolman WB Perturbing the copper(III)−hydroxide unit through ligand structural variation. J. Am. Chem. Soc 2016, 138, 356–368. [PubMed: 26693733]

(46). Wu A; Masland J; Swartz RD; Kaminsky W; Mayer JM Synthesis and characterization of ruthenium bis(β-diketonato) pyridine-imidazole complexes for hydrogen atom transfer. Inorg. Chem 2007, 46, 11190–11201. [PubMed: 18052056]

(47). Ramírez-Solís A; Bartulovich CO; Chciuk TV; Hernández-Cobos J; Saint-Martin H; Maron L; Anderson WR; Li AM; Flowers RA Experimental and theoretical studies on the implications of halide-dependent aqueous solvation of Sm(II). J. Am. Chem. Soc 2018, 140, 16731–16739. [PubMed: 30412400]

(48). Wedal JC; Evans WJ A rare-earth metal retrospective to stimulate all fields. J. Am. Chem. Soc 2021, 143, 18354–18367. [PubMed: 34677044]

(49). McCarthy BD; Martin DJ; Rountree ES; Ullman AC; Dempsey JL Electrochemical reduction of Brønsted acids by glassy carbon in acetonitrile—implications for electrocatalytic hydrogen evolution. Inorg. Chem 2014, 53, 8350–8361. [PubMed: 25076140]

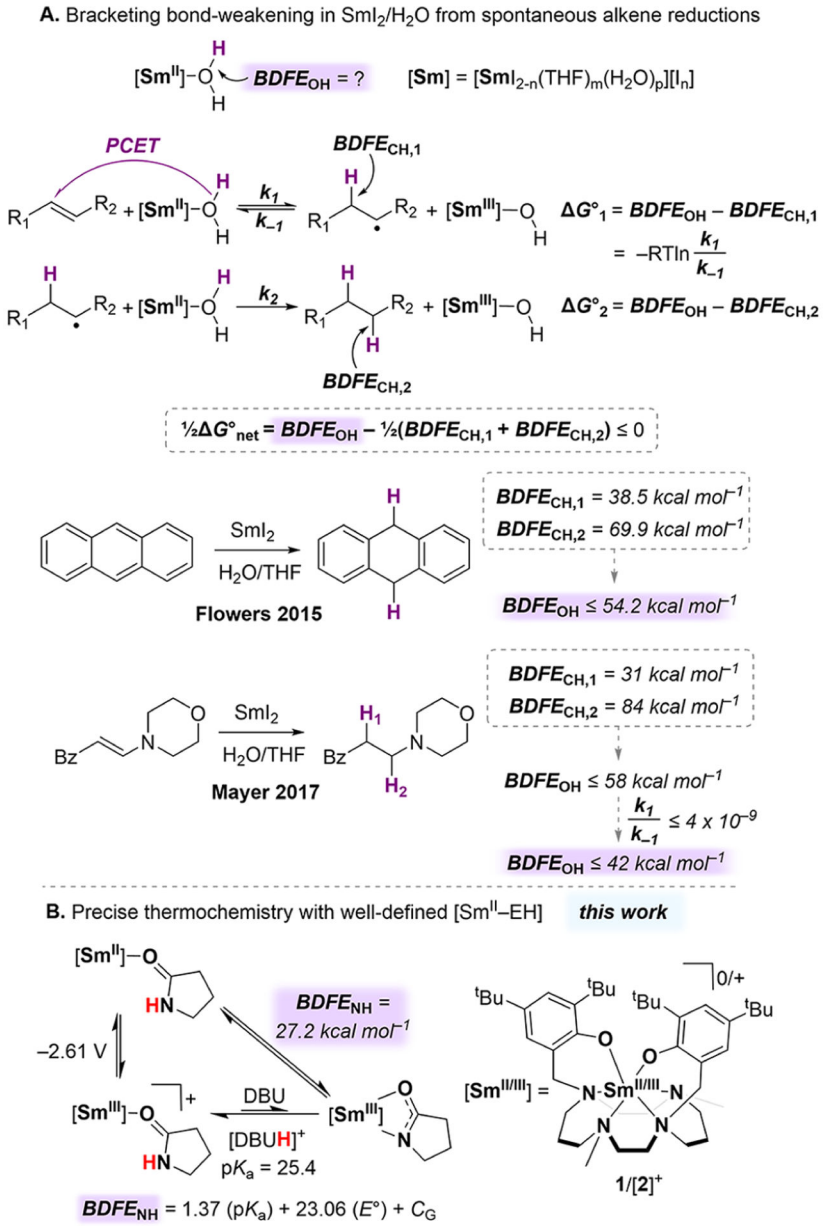

Figure 1.
Quantification of coordination-induced bond weakening at Sm^{II}.

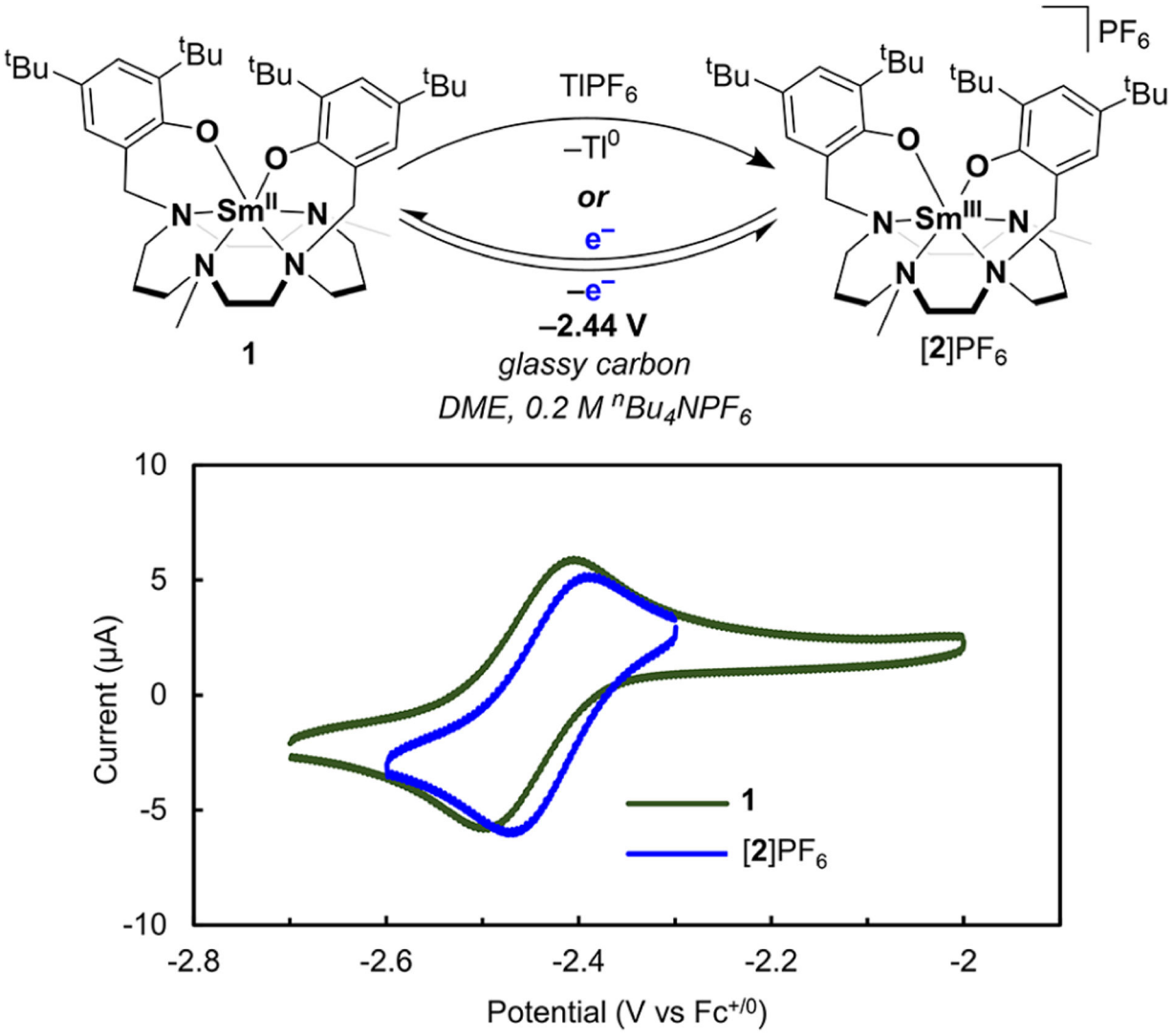

Figure 2.

Chemical and electrochemical conversion between **1** and [**2**]PF_6. CVs of **1** (green, 1 mM) and [**2**]PF_6 (blue, 1 mM) were recorded at 100 mV s^{-1} in DME containing 0.2 M ^{n}Bu$_4$NPF$_6$ with a glassy carbon working electrode, platinum wire counter, and a $Ag^{+/0}$ pseudoreference electrode.

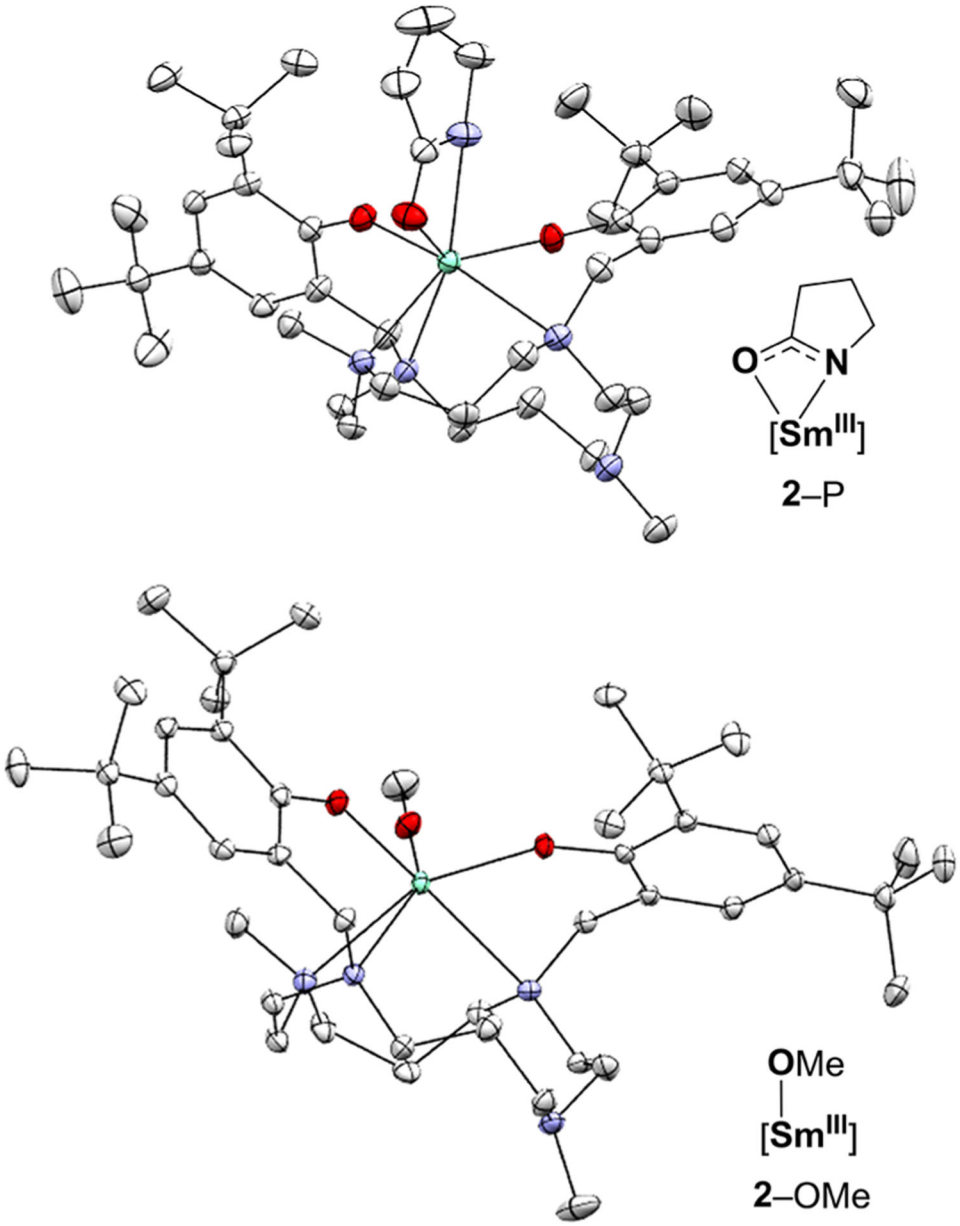

Figure 3.

Solid-state structures of **2**-P and **2**-OMe with thermal ellipsoids set at 50% probability. Hydrogen atoms and co-crystallized solvents are omitted for clarity.

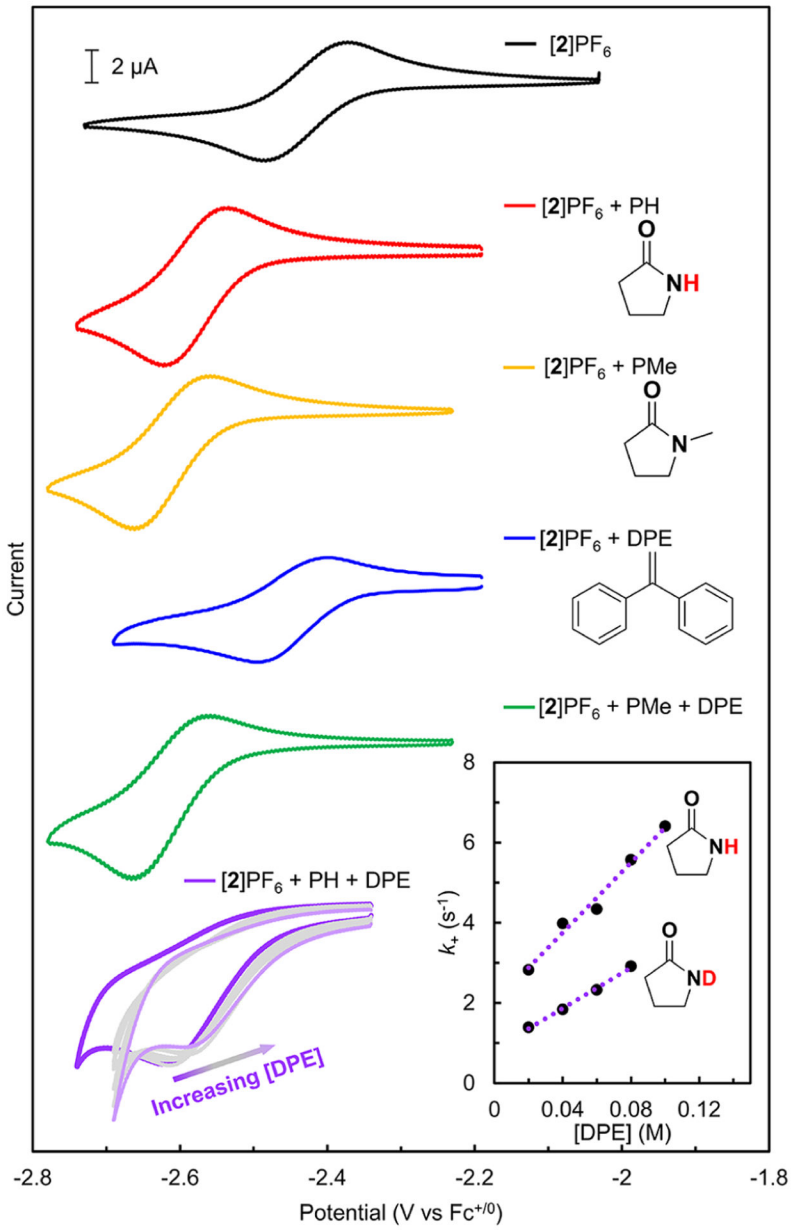

Figure 4.

CVs of [**2**]PF_6 (1 mM) in the presence of combinations of PH (30 mM), PMe (30 mM), and/or DPE. The concentration of DPE is 20 mM in the blue trace and ranges from 20 to 160 mM in the purple traces. CVs were recorded at 100 mV s^{-1} in DME containing 0.2 M $^{n}Bu_4NPF_6$ with a glassy carbon working electrode, platinum wire counter, and $Ag^{+/0}$ pseudoreference electrode. The inset shows the plots used to extract the KIE for the reaction of **1**-PH with DPE.

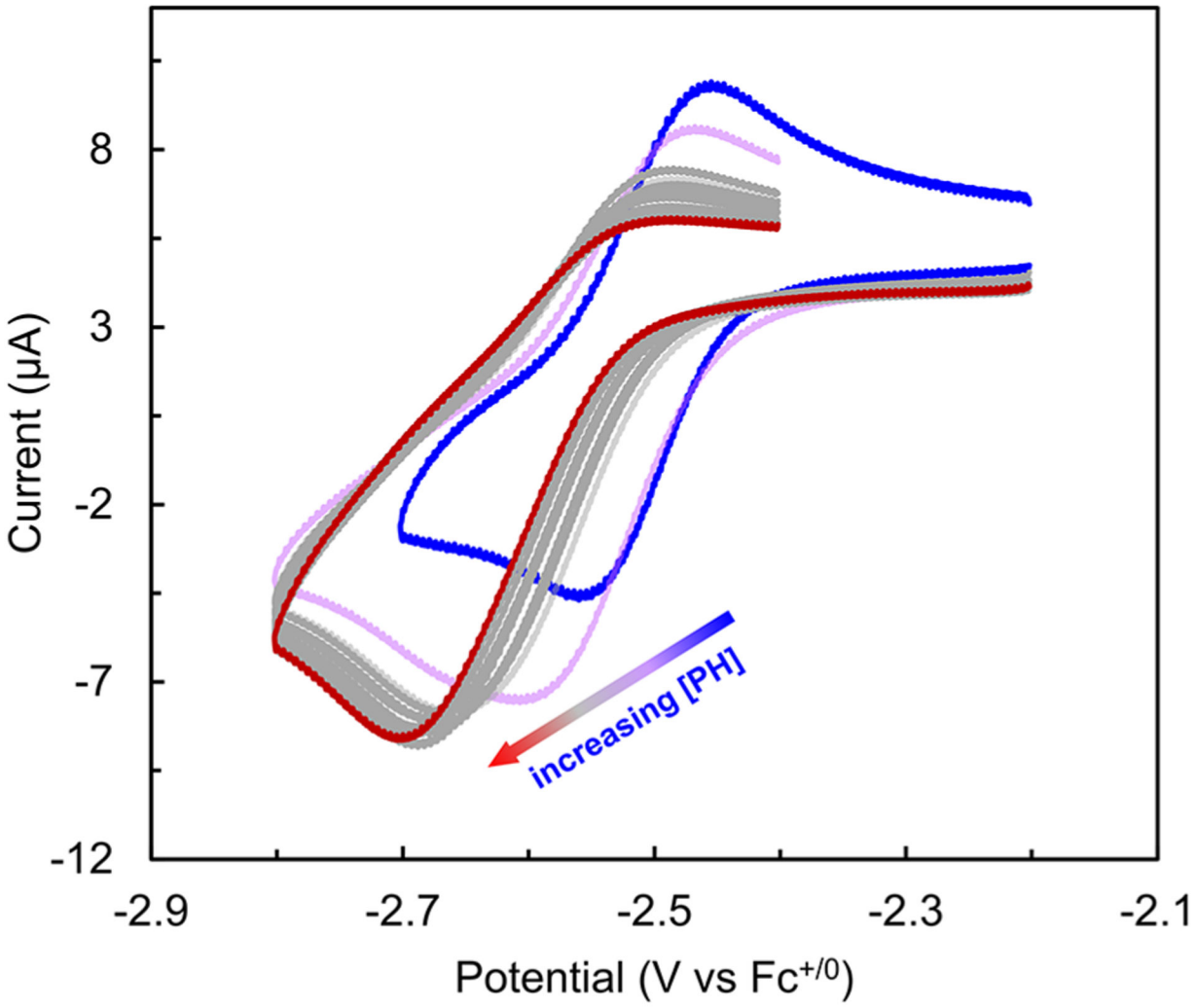

Figure 5.

CV titration of the Sm^{III} cation [**2**-NCMe]PF_6 (1 mM, blue trace) with PH (1−15 equiv) at 100 mV s^{-1} in CH_3CN containing 0.1 M $^{n}Bu_4NPF_6$ with a glassy carbon working electrode, platinum wire counter, and $Ag^{+/0}$ pseudoreference electrode.

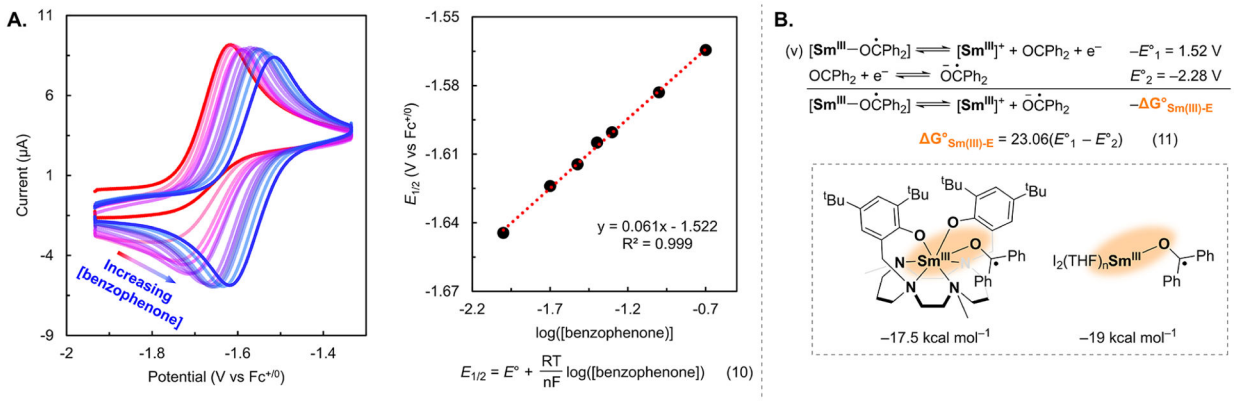

Figure 6.

(A) CV titration of the Sm^{III} cation [**2**]PF_6 (1 mM) with benzophenone (1−200 equiv) and plot of $E_{1/2}$ as a function of benzophenone concentration fitting eq 10. CVs are recorded at 100 mV s^{-1} in DME containing 0.2 M $^{n}Bu_4NPF_6$ with a glassy carbon working electrode, platinum wire counter, and $Ag^{+/0}$ pseudoreference electrode. (B) Thermochemical cycle used to determine $\Delta G°$Sm(III)−E for [**2**-$OCPh_2$] and comparison with $\Delta G°$Sm(III)−E reported for the analogous SmI_2-based species, which we represent for simplicity as $I_2(THF)_nSm{-}OCPh_2^{\cdot}$.[6]

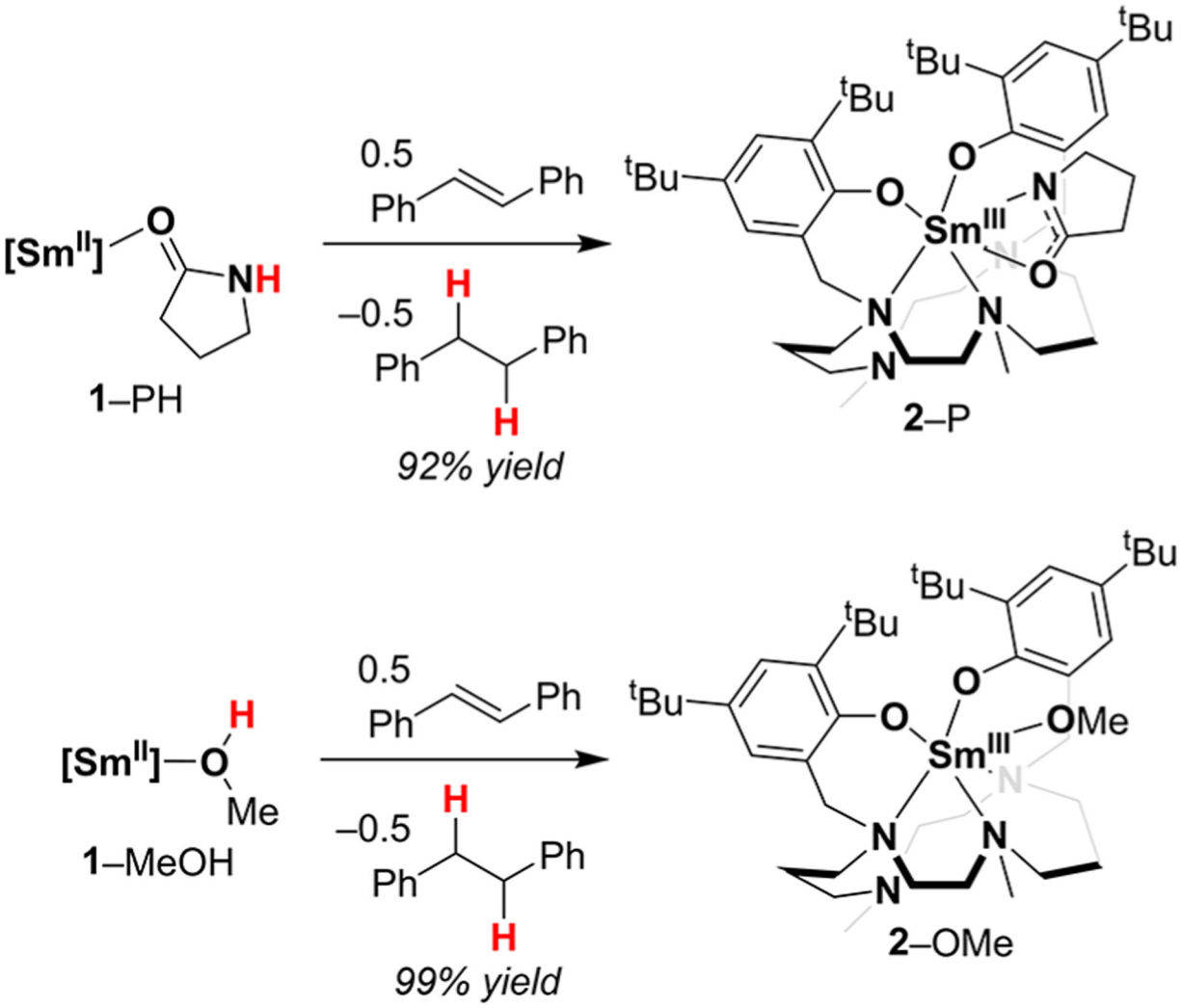

Scheme 1.
Reactivity of 1-PH and 1-MeOH with *trans*-Stilbene to Generate 2-P and 2-OMe

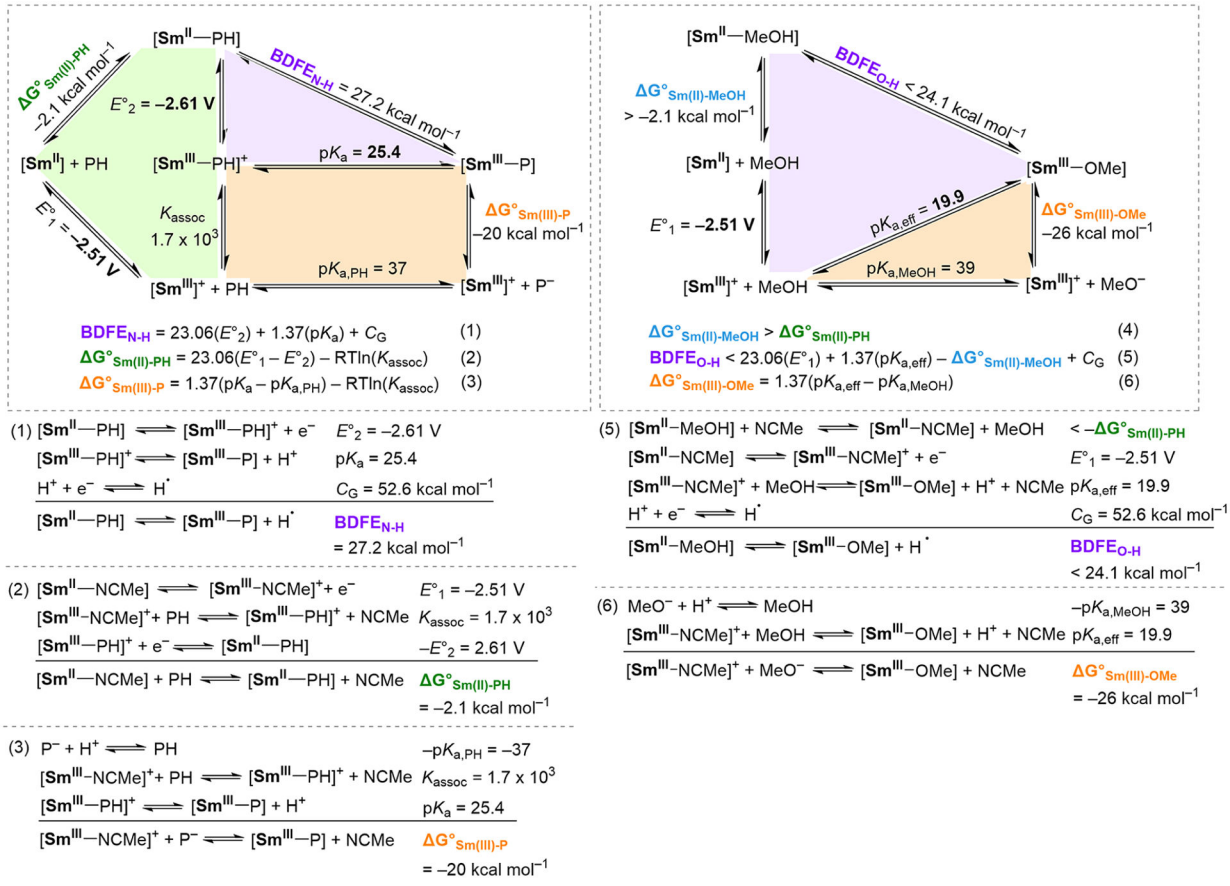

Scheme 2.
Summary of Thermochemical Cycles and Equations

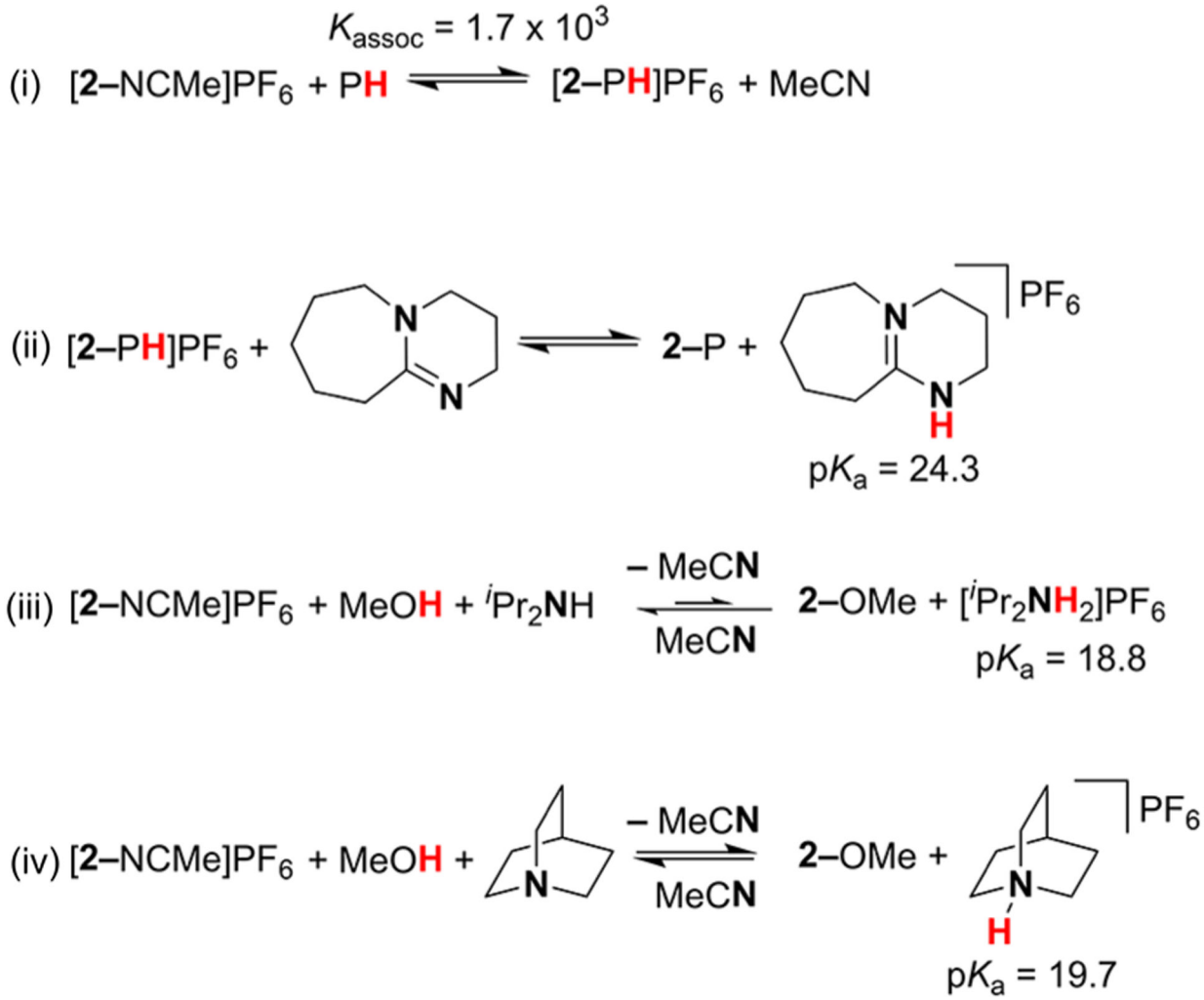

Scheme 3.
Equilibria Relevant to pK_a Determinations

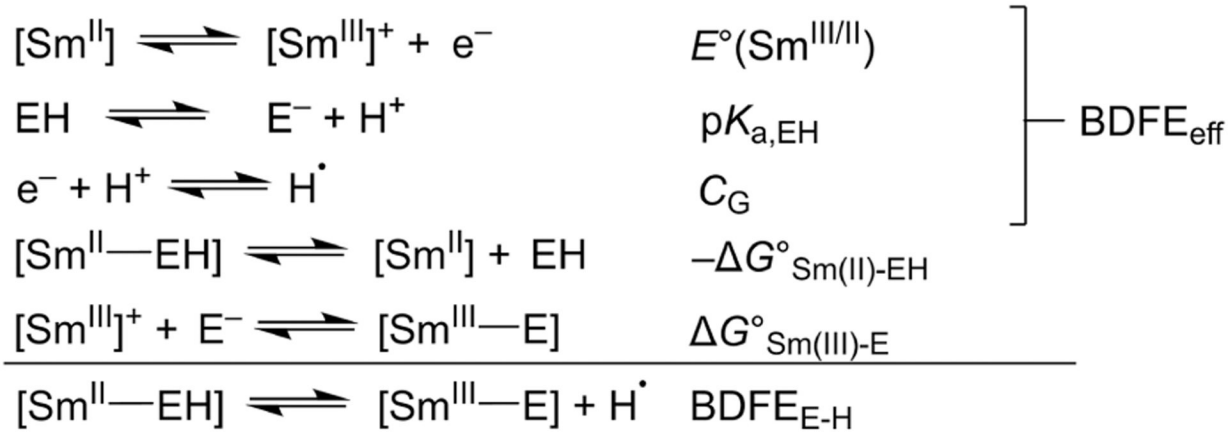

$$\mathrm{BDFE_{eff}} = 23.06(E^\circ(\mathrm{Sm^{III/II}})) + 1.37(\mathrm{p}K_{\mathrm{a,EH}}) + C_{\mathrm{G}} \quad (7)$$

$$\mathrm{BDFE_{E\text{-}H}} = \mathrm{BDFE_{eff}} - \Delta G^\circ_{\mathrm{Sm(II)\text{-}EH}} + \Delta G^\circ_{\mathrm{Sm(III)\text{-}E}} \quad (8)$$

$$\Delta\mathrm{BDFE} = \mathrm{BDFE_{eff}} - \mathrm{BDFE_{E\text{-}H}} = \Delta G^\circ_{\mathrm{Sm(II)\text{-}EH}} - \Delta G^\circ_{\mathrm{Sm(III)\text{-}E}} \quad (9)$$

Scheme 4.
Contributions to BDFE $_{\mathrm{E-H}}$

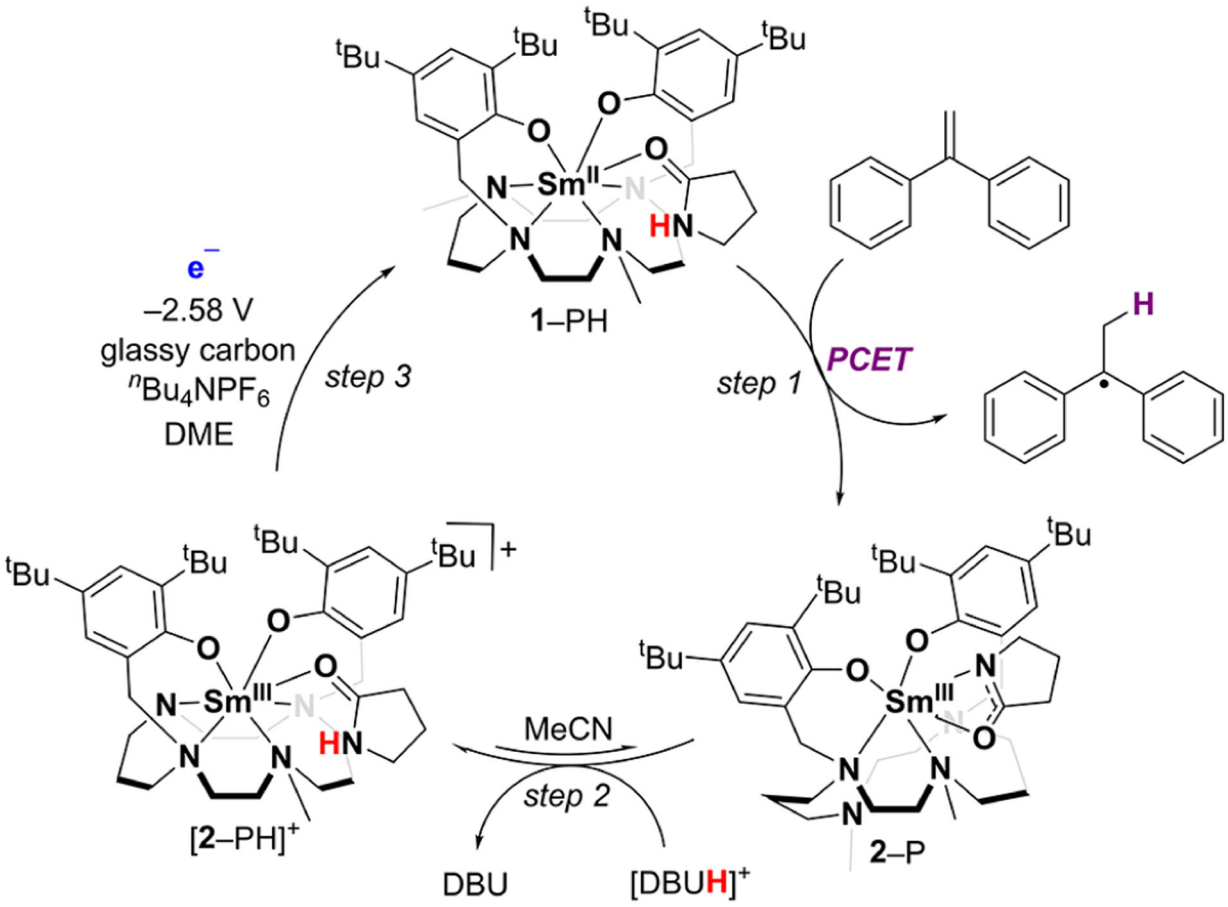

Scheme 5.
Steps Demonstrated in a Hypothetical Sm-Mediated Electrocatalytic PCET Cycle